OAK RIDGE INSTITUTE
FOR SCIENCE AND EDUCATION
Shaping the Future of Science

October 31, 2022

Kimberly Conway
U.S. Nuclear Regulatory Commission
11545 Rockville Pike
Mail Stop T8F5
Rockville, MD 20852

SUBJECT: **CONTRACT NO. DE-SC0014664**
ESTIMATING SCAN MINIMUM DETECTABLE ACTIVITIES OF DISCRETE RADIOACTIVE PARTICLES
DCN: 5364-TR-01-D1

Dear Ms. Conway:

The Oak Ridge Institute for Science and Education (ORISE) is pleased to provide the enclosed technical basis detailing the methods and results for estimating scan minimum detectable activities of discrete radioactive particles (DRPs). NRC comments have been addressed in this revised draft version. ORISE will wait to finalize until after NRC's DRP workshop scheduled for November 3, 2022, to determine if any feedback warrants additional revisions.

Please feel free to contact me at 865.576.6659 or Nick Altic at Nick.Altic@orau.org if you have any questions.

Sincerely,

Erika N. Bailey

Erika Bailey
Survey Projects Manager
ORISE

NAA:enb

Attachment

Electronic distribution: G. Chapman, NRC; D. Brown, NRC; C. Barr, NRC; N. Altic, ORISE; D. King, ORISE; D. Hagemeyer, ORISE; File/5364

Distribution approval and concurrence:	Initials
Group Manager Review	

THIS PAGE INTENTIONALLY LEFT BLANK.

ESTIMATING SCAN MINIMUM DETACTABLE ACTIVITIES OF DISCRETE RADIOACTIVE PARTICLES

Prepared by:
N. Altic and D. King

REVISED DRAFT, D1

TECHNICAL REPORT

Prepared for the:
U.S. Nuclear Regulatory Commission

October 2022

Further dissemination authorized to NRC only; other requests shall be approved by the originating facility or higher NRC programmatic authority.

This document was prepared for the U.S. Nuclear Regulatory Commission (NRC) by the Oak Ridge Institute for Science and Education (ORISE) through Interagency Agreement 31310021S0033 between the NRC and the U.S. Department of Energy (DOE). ORISE is managed by Oak Ridge Associated Universities under DOE contract number DE-SC0014664.

ORAU provides innovative scientific and technical solutions to advance research and education, protect public health and the environment and strengthen national security. Through specialized teams of experts, unique laboratory capabilities and access to a consortium of more than 100 major Ph.D.-granting institutions, ORAU works with federal, state, local and commercial customers to advance national priorities and serve the public interest. A 501(c) (3) nonprofit corporation and federal contractor, ORAU manages the Oak Ridge Institute for Science and Education (ORISE) for the U.S. Department of Energy (DOE). Learn more about ORAU at www.orau.org.

NOTICES

The opinions expressed herein do not necessarily reflect the opinions of the sponsoring institutions of Oak Ridge Associated Universities.

ESTIMATING SCAN MINIMUM DETACTABLE ACTIVITIES OF DISCRETE RADIOACTIVE PARTICLES

1. INTRODUCTION

The traditional method for estimating a scan minimum detectable concentration (MDC) is described in NUREG-1507 (U.S. Nuclear Regulatory Commission [NRC] 2020), which assumes surveyors pass a detector directly over a specified volume of contaminated surface soil. (The NUREG-1507 approach is deemed the standard model in this report.) While survey planners can follow the NUREG guidelines and adjust input variables to match site-specific conditions, the guidance does not address challenges associated with discrete radioactive particles (DRPs). This technical report, therefore, presents scan minimum detectible activity (MDA) calculations for DRPs. In addition, the NUREG scan MDC method assumes a surveyor will pause directly over a small area (or volume) of contamination, and this assessment evaluates impacts on the scan MDA when: 1) the surveyor's/detector's path does not pass directly over the DRP and 2) the DRP is covered with clean soil.

2. CONCEPTUAL MODEL

This evaluated conceptual model for the calculation of DRP scan MDAs consisted of the traditional surveyor paradigm whereby an individual uses a hand-held gamma detector to assess the presence of elevated direct radiation based on the instrument's audio response.

This technical approach also considered the possibility that DRPs can be covered with clean soil by considering cover depths of 0 cm, 7.5 cm, 15 cm, and 30 cm. Obviously, DRPs may be present at any depth, but specific values are selected to limit calculation times. Calculations are also limited to the following potential contaminants: Co-60, Cs-137, Th-232, and Am-241—only Co-60 and Cs-137 are evaluated at a depth of 30 cm. Finally, only an unshielded 2-inch by 2-inch sodium iodide (2×2 NaI) detector is considered. In summary, the two conceptual models considered in this technical report include the following:

- Optimistic and pessimistic (offset) survey pathways using a 2×2 NaI detector,
- Co-60, Cs-137, Th-232, and Am-241 DRPs,
- Detector heights of 7.5 cm and 10 cm,

- Soil cover depth of 0 cm, 7.5 cm, 15 cm, and 30 cm (calculations for a depth cover of 30 cm was only performed for Co-60 and Cs-137), and
- Surveyor scan speed of 0.25 m/s, 0.5 m/s, and 1 m/s

The physical setting of the surveyor and surrounding environment was modeled in a three-dimensional Cartesian coordinate system (i.e., X, Y, and Z axes). The hypothetical surveyor is standing in the +Z direction and walking the +Y direction with constant velocity, v in meters per second (m/s). While the surveyor progresses in the forward (+Y) direction, the detector moves side-to-side (in the ±X axis), maintaining a constant ground-to-detector distance. Detector position through the surveyor's transect was modeled as a sine curve, which represents the flat, serpentine motion of the detector during a survey transect. In order to adequately represent the sine curve, coordinates specifying the location of 200 evenly spaced points along the sine curve as the surveyor moves 2 meters (6.6 ft) in the Y-direction were generated. Viewing the detector position in the XY-plane (looking into the –Z direction), the position along a portion of the surveyor's transect is illustrated in Figure 2.1. The detector position (represented by each dot in Figure 2.1) occurs at a specific time based on the surveyor's forward velocity, assuming the time between each dot is equivalent. For example, assume that the detector starts at location (-0.5 m, -1.0 m), the surveyor velocity is 1.0 m/s, and the surveyor will traverse the 2-m interval displayed in Figure 2.2 in 2 seconds. There are 200 points depicted in Figure 2.1, so the time between each point represents 0.01 seconds.

The standard model (traditional NUREG-1507 approach) assumes that detection efficiency is maximized because the detector is perfectly positioned over the source center and the source is at the surface (i.e., no soil cover). This approach may be a reasonable approximation for volumetric sources, but may be much less reasonable for DRPs. Therefore, this technical approach considers the possibility that the detector will pass to the side of the DRP (i.e., by some offset). Figure 2.1 illustrates the "optimistic" serpentine path, where the detector eventually passes directly over the DRP, and the "pessimistic" or offset path, where the detector follows a similar path though the detector-to-DRP distance is maximized—scan MDAs are estimated in this technical report for both the optimistic and the pessimistic DRP locations.

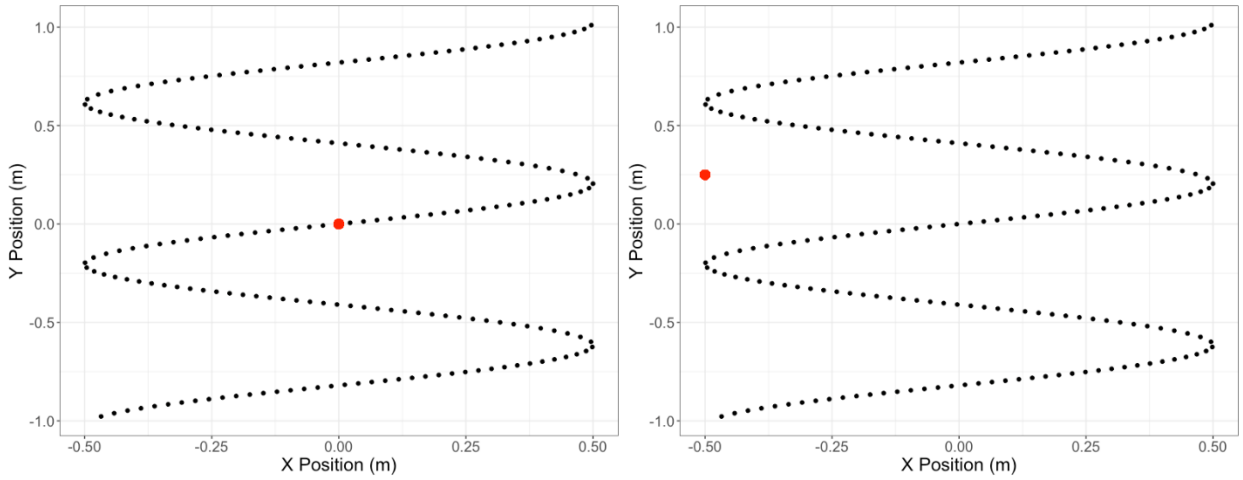

Figure 2.1. a) Optimistic scenario where detector passes directly over the source and b) pessimistic scenario where detector is furthest distance from surveyor transect. The surveyor is walking in the +Y direction and swinging the NaI detector in the ±X-axis. The surveyor is standing in the direction of the +Z axis. (The red dot indicates source location.)

3. METHODS

The standard model includes an efficiency term whereby a source of some specified strength (typically calculated in MicroShield®) produces some exposure rate (in μR/h). Literature for the detector manufacturer typically provides the detector's response in counts per minute (cpm) for a given μR/h, so the modeler can estimate the detector response for a given source strength. This approach is not practical for a DRP model. The exposure rate estimate for the standard model (i.e., using MicroShield) is for a fixed location directly above the center of the volume source. While this approximation may by acceptable for a volume source, it is not acceptable for a DRP. That is, the standard model tacitly accepts that this maximized response will be uniform for the whole observation interval. This is unrealistic, at best, for a DRP because the DRP footprint is diminishingly small and the response varies with even a small offset. Therefore, a different approach is required. There are two steps for assessing DRP scan MDAs: 1) determining the detector efficiency at various points along the surveyor's transect and 2) calculating the response from the DRP that corresponds to the instrument's audio output used by the surveyor to assess the presence of a DRP—known as the minimum detectable count rate (MDCR) in the standard model.

3.1 DETECTOR EFFICIENCY

Fortunately, calculating the detector response at each location depicted in Figure 2.1 is straightforward relative to that of a volumetric source. If a detector response function can be modeled as a function of lateral offset, then detector response can be calculated at any detector position along the surveyor's transect. Monte Carlo N-Particle (MCNP®) transport code, version 6.2, was used to calculate detector response to a point source at 5-cm lateral offset positions. A graphical depiction of the MCNP model is illustrated in Figure 3.1. That is, MCNP calculates the "pulse-height" of each photon that deposits energy in the NaI crystal. Summing all of the photon pulse-heights yields the NaI response in units of counts per source strength (i.e., counts/decay).

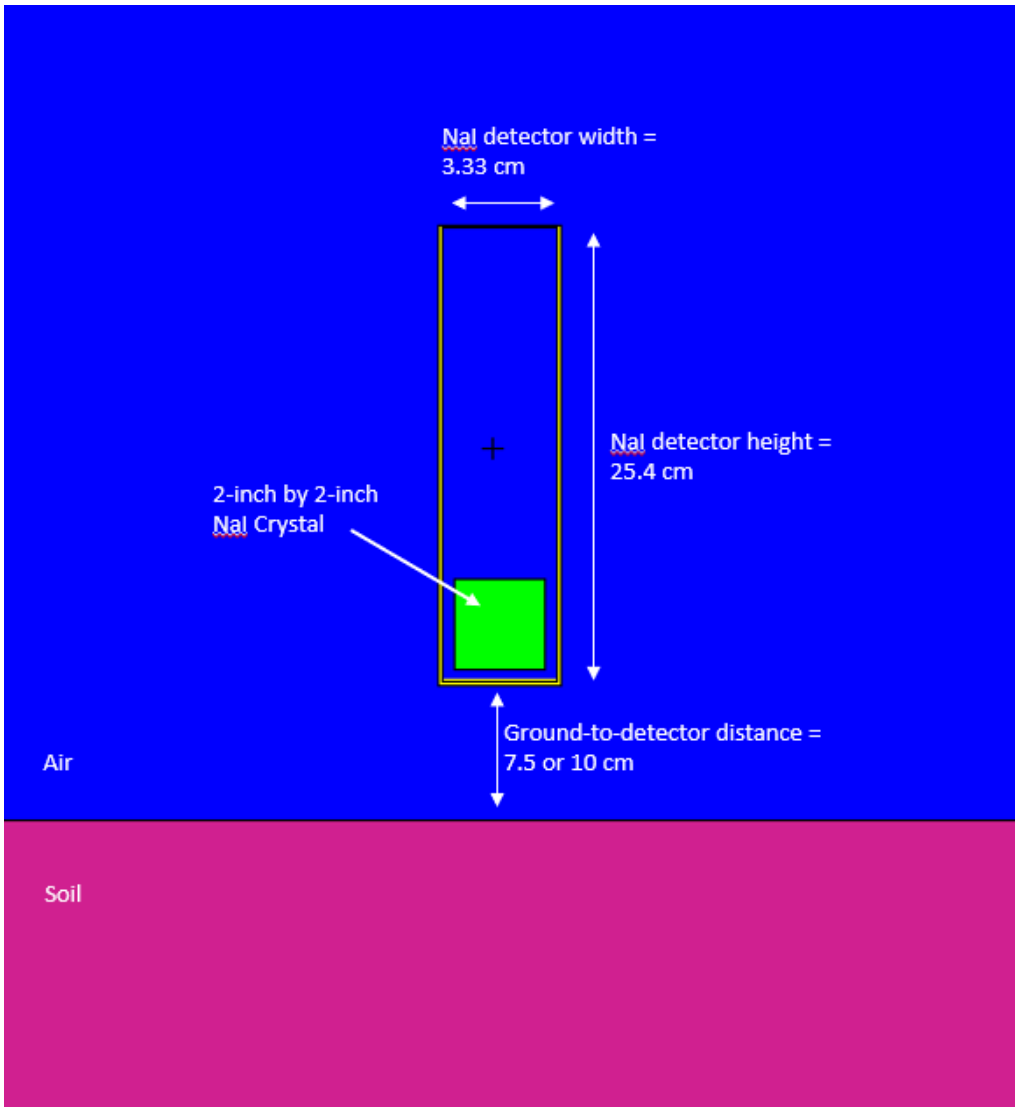

Figure 3.1. MCNP geometry for DRP efficiency calculations (blue=dry air, magenta=soil, green=NaI crystal, yellow=aluminum).

In general, the MCNP results had a relative error less than five percent. Relative error increased with increasing soil depth and detector offset, which is expected. Efficiency evaluations for Co-60 and Cs-137 at a depth of 30 cm had relative errors greater than 10% for offsets greater than 90 cm. Calculations Am-241 efficiency at soil depths of 7.5 cm and greater would not converge. That is, the soil sufficiently attenuated Am-241 gammas such that running additional MCNP histories would not provide improved results. Therefore at-depth efficiency curves were not generated for Am-241.

The resulting 5-cm incremental response data were fit with a log-logistic survey using the drc package in the R computer code, version 4.1.2. Figure 3.2 illustrates example efficiency curves for Co-60 under the various modeling scenarios. The efficiency term for a given soil cover depth is described by the equation:

$$EFF(\delta) = c + \frac{(d-c)}{\left(1+\exp\left(b\left(ln(\delta)-ln(e)\right)\right)\right)^{f}} \qquad \text{(Eq. 3-1)}$$

Where:

EFF(δ) = NaI detector response efficiency function (counts/decay),
δ = lateral distance or offset from the detector to the DRP (cm), and
b, c, d, e, f = coefficients for the log-logistic curve.

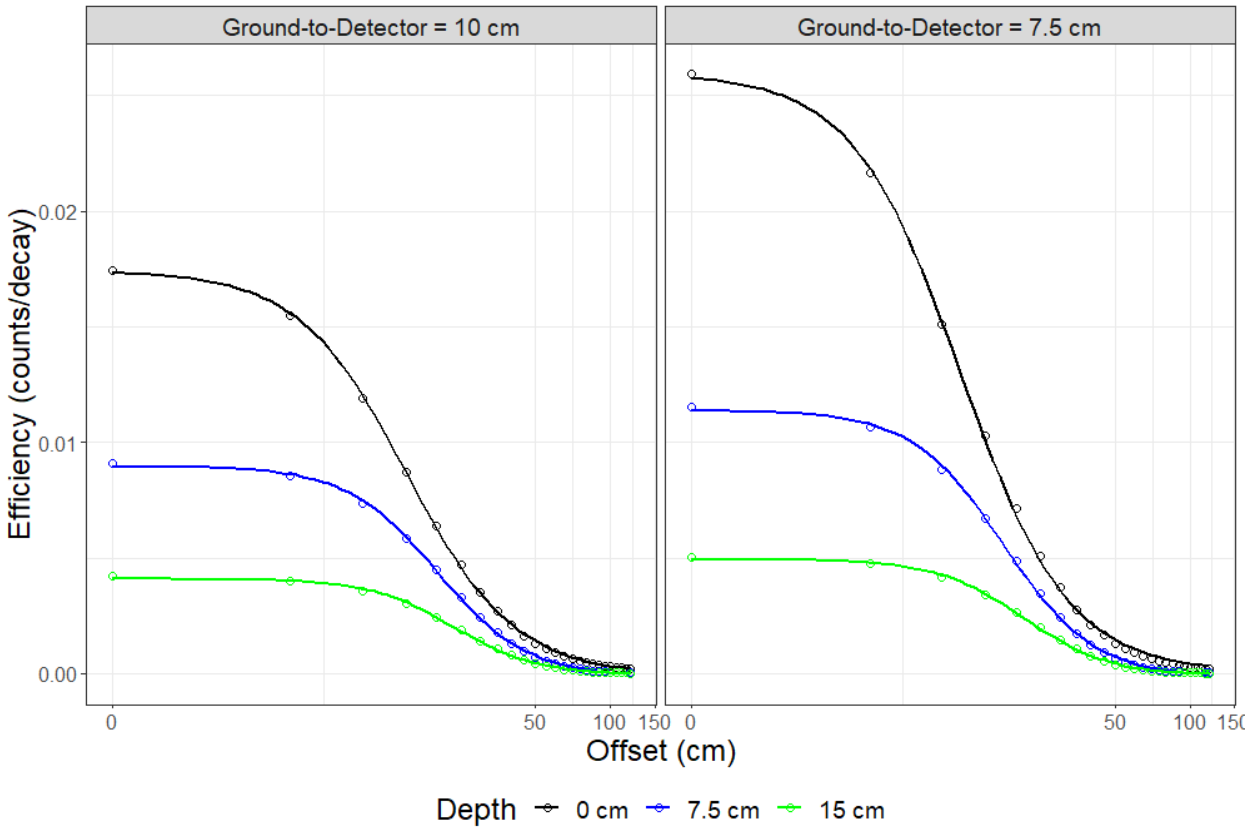

Figure 3.2. Co-60 Efficiency curves as a function of detector offset for the evaluated detector ground-to-detector distance

Fit coefficients for the log-logistic curve depicted in Figure 3.2 are presented in Table 3.1 below.

Table 3.1. Fit Parameters for the log-logistic functions describing detector efficiency for various particle depths and source-to-detector distances

Fit Parameter	Ground-to-Detector Distance = 7.5 cm			Ground-to-Detector Distance = 10 cm		
	Surface DRP	7.5 cm DRP depth	15 cm DRP depth	Surface DRP	7.5 cm DRP depth	15 cm DRP depth
b	1.75E+00	1.86E+00	1.91E+00	1.78E+00	1.86E+00	1.90E+00
c	-4.60E-05	-8.83E-06	6.73E-06	-2.18E-05	5.06E-06	8.52E-06
d	2.59E-02	1.15E-02	5.03E-03	1.74E-02	9.11E-03	4.19E-03
e	1.48E+01	3.00E+01	4.17E+01	1.86E+01	3.54E+01	4.68E+01
f	1.30E+00	2.24E+00	2.92E+00	1.32E+00	2.40E+00	3.04E+00

SD = Source-to-detector distance

Detector counts per activity efficiency values are estimated for each combination of detector position along the path, DRP depth, and radionuclide. The MCNP model used here replaces the standard model's efficiency terms with a probability of interaction. The emitted photon could travel

through soil (if cover is modeled), through air, through the metal casing, and into the sensitive NaI volume where the pulse is created. Any single photon has a low probability of completing this path and generating a pulse—a small number of counts per decay—especially when considering cover depth and the detector offset. In any case, this probability of generating a pulse is interpreted as the detector's efficiency. Simply, the *EFF(δ)* term represents the fraction of the photons that reach the detector and generate a pulse when the detector is at a given location.

In addition to the MCNP calculation approach, similar efficiency curves were generated for Co-60 and Cs-137 using MicroShield®, v7.02. MicroShield calculates exposure rate from a radiation source under user-defined geometries, therefore, the output must be converted to instrument response using the processes presented in Section 6.2.5 of NUREG-1507 (NRC 2020).

3.2 TOTAL INTEGRATED RESPONSE AND SCAN MDA

Scan MDAs can be calculated using the *EFF(δ)* term determined from a single, fixed position, which is similar to the standard model per NUREG-1507 using MicroShield, or the function can be manipulated to approximate the response for a detector in motion. The latter approach is taken here. Therefore, the next step is to calculate the detector response at each point in Figure 2.1 using the fitted MCNP data, as described by Eq. 3-1. Recall that the spacing between each point along the path (Figure 2.1) represents an equal time increment. Thus, for a surveyor velocity of v = 0.5 m/s, the interval between each point represents 0.02 s [(2 m/0.5 m/s)/200 points = 0.02 s]. Detector response at each point can be reframed as a function of time. Therefore, the detector efficiency is implicitly a function of time. The response along the surveyor's transect is given by:

$$R(\delta, t) = K \times A \times EFF(\delta, t) \qquad \text{(Eq. 3-2)}$$

Where:

R(δ,t) = NaI detector response efficiency function (cpm/μCi) at a specified point/time (t),
EFF(δ,t) = NaI detector response efficiency function (counts/decay) at a specified point/time (t),
K = unit conversion factor (1 decay/sec/Bq × 37,000 Bq/μCi × 60 sec/min), and
A = the DRP activity (μCi).

Figure 3.3 illustrates the detector response for a 2-m portion of the surveyor's transect as a function of time. The characteristic shape of the NaI detector response is represented by a narrow Gaussian-like peak. A response function for the typical NUREG-1507 0.25-m^2 source would take more of a

uniform shape. In other words, detector response would be relatively uniform as the surveyor travels over the source compared to the response from passing over a DRP. Because of the difference in response, the implicit standard-model assumption of a constant detector response (over the observation interval for a disk source) does not hold for a DRP. Therefore, a total integrated response—over the DRP observation interval—is needed.

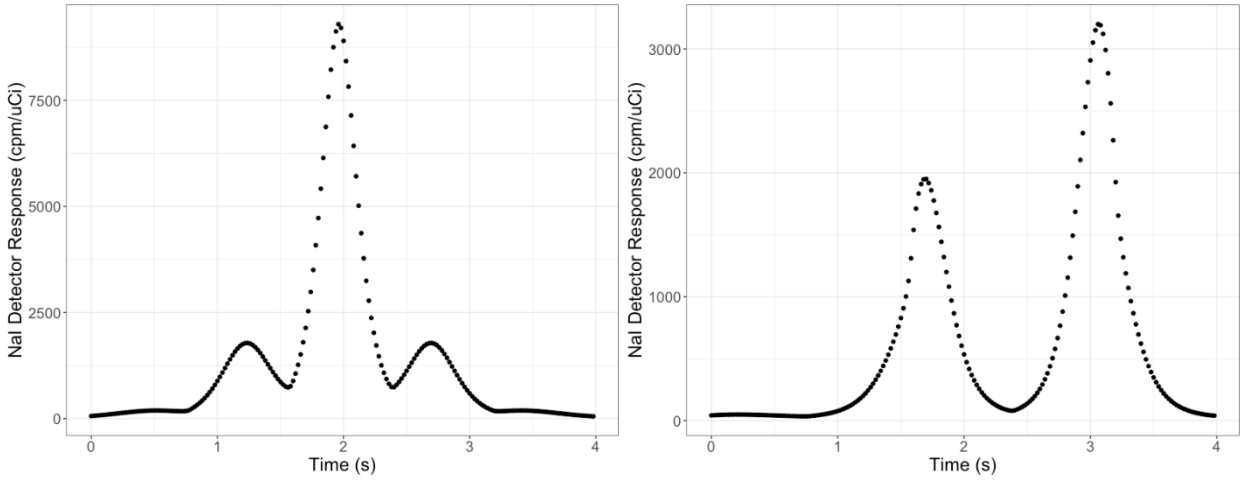

Figure 3.3. NaI Detector response as a function of surveyor time for the a) optimistic scenario and b) pessimistic scenario

Selection of the observation interval requires additional consideration. The observation interval cannot be a fixed value because the surveyor is not mentally integrating the ratemeter audio output over a previously defined interval. For example, under the optimistic scenario, the surveyor hears a rapid rise/decease in audio output. The sharp increase/decrease occurs over a period of approximately 0.75 seconds. Because the real-time audio response is proportional to the NaI detector response, the total integrated response of the largest peak in Figure 3.3 (over an interval of 0.75 sec) is directly related to the instrument's audio output.

Mathematically, the total integrated response over the observation interval is the integral of the response function, given by:

$$IR(i) = \int_i R(\delta, t)\, d\delta\, dt \qquad \text{(Eq. 3-3)}$$

Because the lateral offset (δ) is no longer a variable, Eq. 3-3 can be simplified to:

$$IR(i) = K \times A \times \int_{tmin}^{tmax} R(t)\, dt \qquad \text{(Eq. 3-4)}$$

Where t_{min} and t_{max} are the lower and upper bounds of the observation interval, respectively. Rather than attempting to fit an equation to the response function depicted in Figure 3.3, the integral in Eq. 3-4 is calculated using the trapezoid rule—which approximates the area under a curve by subdividing the area into a number of small trapezoids—using the DescTools package in R. The area of trapezoids are summed from t_{min} to t_{max}, where t represents time—on the x-axis of Figure 3.3. The difference ($t_{max} - t_{min}$) represents the observation interval. For example, under the optimistic scenario, the first local minimum before the global maximum was selected for t_{min}, approximately 1.6 s. Similarly, t_{max} is the first local minimum occurring after the global maximum, approximately 2.4 s. As indicated in the prior discussion, the observation interval is dependent on the shape of the detector response curve. The concept of a dynamic observation interval differs from the traditional fixed observation interval; however, this difference is justified as the surveyor is not mentally integrating the audio response over the observation interval.

The scan MDC equation—for land area gamma scans—presented for the standard model in NUREG-1507 can be slightly reformatted for a DRP as:

$$scan\ MDA = \frac{MDCt}{\sqrt{p} \cdot IR} = \frac{d' \sqrt{b_i}}{\sqrt{p} \cdot IR} \qquad \text{(Eq. 3-5)}$$

Where:

scan MDA = scan minimum detectable activity (μCi),
MDCt = minimum detectable counts (counts),
d' = index of sensitivity, 1.64 used here (unitless),
b_i = background counts during observation interval (counts); a background count rate of 10,000 cpm was assumed,
i = observation interval (seconds),
IR = integrated detector response [*R(δ, t)*] over observation interval (cpm/μCi s), and
p = surveyor efficiency, 0.5 used here (unitless).

Note, the scan MDA equation above differs from Equation 6.11 in NUREG-1507 by the removal of (60/*i*), which corrects MDCt to the MDCR in Equation 6.11. The MDCR term is unnecessary in this method because the NaI detector response is integrated over the observation interval.

In addition to the different radionuclides of interest, the ground-to-detector distances, and source depths, the scan MDA calculations were performed for a surveyor velocity of 0.5 m/s and 1.0 m/s. The surveyor velocity dictates the timing between detector position (Figure 2.1)—as previously mentioned, for a velocity of 0.5 m/s, each point represents 0.02 m/s and, for a velocity of 1.0 m/s, each point represents 0.01 s.

3.3 MICROSHIELD ANALYSIS

MCNP may not be a viable option for performing the DRP efficiency calculations discussed in Section 3.1 for all MARSSIM practitioners. Therefore, efficiency curves for a subset of radionuclides—Co-60 and Cs-137—were generated using MicroShield and calculation methods similar to those presented previously were used to determine scan MDAs. MicroShield derived scan MDAs for Co-60 and Cs-137 were evaluated at under the same conditions as their MCNP-calculated analogue. Equations describing scan MDA for this analysis have the same form as those presented in the previous sections. However, because the instrument response is not directly evaluated using MicroShield, the calculated exposure rate must be converted to a detector response—in units of cpm—using the count-rate per micro-R per hour (CPMR) values presented in NUREG-1507 (NRC 2020). Values of the CPMR for Cs-137 and Co-60 are 900 and 429 cpm/μR/hr, respectively.

3.4 MCNP MODEL QC

As a quality control (QC) check of modeled results, an experiment was performed by collecting measurements using a 2×2 NaI detector and a small, 4.76-μCi Co-60 source. As illustrated in Figure 3.5, the 2×2 NaI detector was maintained at a constant height of 10 cm above a wooden table as the source was moved at 5-cm increments. The detector response in cpm was recorded at each increment to be compared against modeled results generated using MCNP. As illustrated, the Co-60 source is small, but not a true point source, and the measurement surface is a wooden countertop and not soil. Therefore, empirical and modeled results were not expected to match exactly, though the empirical results should suggest if the MCNP model is viable and can reasonably be used to estimate scan MDA values.

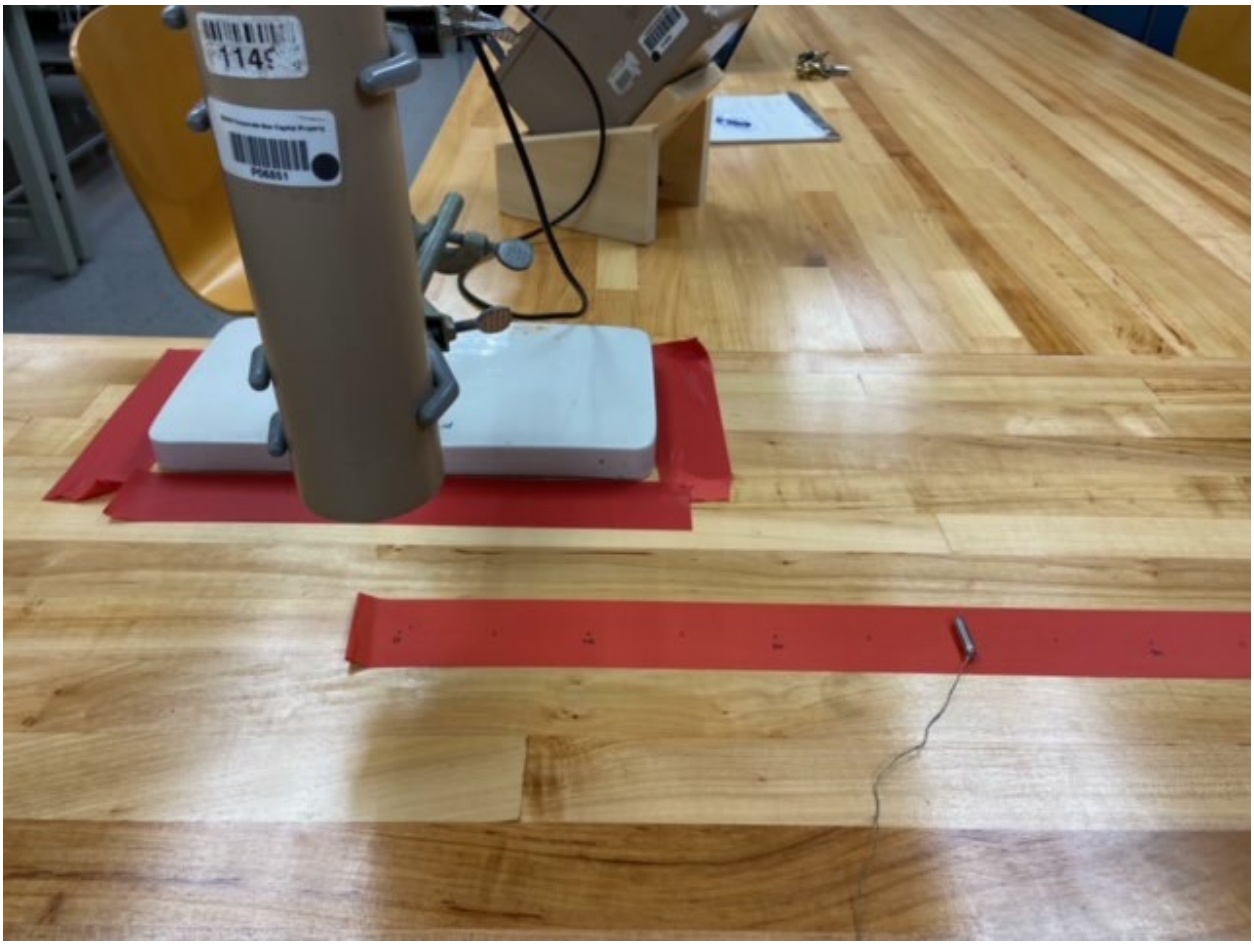

Figure 3.5. Offset experiment using a 4.76 µCi Co-60 source

4. RESULTS AND DISCUSSION

4.1 SURVEYOR SCAN MDA

Table 4.1 presents scan MDA values for all modeled combinations of radionuclide, offset, and depth for a surveyor velocity of 0.25 m/s. "Optimistic" values are provided on the top portion of the table, representing the MDA assuming the detector passes directly over the DRP, as shown in Figure 2.1a. "Pessimistic" values are provided on the bottom portion of the table, representing the MDA assuming the DRP is located within the straight-line path of the surveyor but is positioned at a maximum distance from the detector's serpentine path, as shown in Figure 2.1b. Note that, as a general rule, the pessimistic MDA is approximately four times (range of 1.9 to 5.7, average 4.2) higher than the optimistic MDA. That is, it theoretically takes up to four times the activity to identify contamination while scanning if the detector does not pass directly over the DRP.

Calculations show that Am-241 can only be identified if present on the surface (noting that the first cover depth considered is 7.5 cm or ~3 inches). In general, and as expected, radionuclides with high-energy gammas produce the lowest MDA (are more easily detected), especially when the DRP is covered with soil. The Th-232 DRP is shown to have the lowest surface scan MDA due to the abundance of gamma radiation from thorium series decay products. The Th-232 scan MDA increases more rapidly—relative to Co-60 and Cs-137—as low-energy gamma particles are more effectively shielded by the soil cover.

Table 4.1. DRP scan MDA for various scan conditions and a surveyor velocity of 0.25 m/s (µCi)

Particle Depth in Soil	Radionuclide and Ground-to-Detector Distance							
	Co-60		Cs-137		Th-232		Am-241	
	7.5 cm	10 cm	7.5 cm	10 cm	7.5 cm	10 cm	7.5 cm	10 cm
Optimistic Scenario (Figure 2.1a)								
Surface	0.09	0.11	0.16	0.21	0.04	0.05	0.35	0.45
7.5 cm	0.15	0.18	0.33	0.38	0.12	0.13	-	-
15 cm	0.31	0.34	0.77	0.85	0.29	0.33	-	-
30 cm	1.2	-	4.2	-	-	-	-	-
Pessimistic Scenario (Figure 2.1b)								
Surface	0.37	0.38	0.74	0.75	0.19	0.19	1.7	1.7
7.5 cm	0.70	0.67	1.8	1.6	0.66	0.61	-	-
15 cm	1.2	1.1	3.4	3.2	1.3	1.3	-	-
30 cm	3.4	-	14.1	-	-	-	-	-

"–" indicates the calculation shows the DRP cannot be identified during scans.
All values rounded to two significant digits or the hundredth position.

Table 4.2 presents scan MDAs for a surveyor velocity of 0.5 m/s. Scan MDAs for the various radionuclides and field conditions follow the same trend as the values under the slower surveyor velocity. Unsurprisingly, the higher surveyor velocity yields a higher scan MDA relative to a surveyor velocity of 0.25 m/s—by a factor of approximately 1.4.

Table 4.2. DRP scan MDA for various scan conditions and a surveyor velocity of 0.5 m/s (µCi)

Particle Depth in Soil	Radionuclide and Ground-to-Detector Distance							
	Co-60		Cs-137		Th-232		Am-241	
	7.5 cm	10 cm	7.5 cm	10 cm	7.5 cm	10 cm	7.5 cm	10 cm
Optimistic Scenario (Figure 2.1a)								
Surface	0.12	0.15	0.23	0.29	0.06	0.07	0.50	0.63
7.5 cm	0.22	0.25	0.47	0.54	0.16	0.19	-	-
15 cm	0.43	0.48	1.09	1.21	0.41	0.46	-	-
30 cm	1.7	-	5.9	-	-	-	-	-
Pessimistic Scenario (Figure 2.1b)								
Surface	0.52	0.53	1.0	1.1	0.27	0.28	2.41	2.46
7.5 cm	0.99	0.94	2.5	2.3	0.93	0.86	-	-
15 cm	1.7	1.6	4.9	4.6	1.9	1.8	-	-
30 cm	4.9	-	19.9	-	-	-	-	-

"–" indicates the calculation shows the DRP cannot be identified during scans.
All values rounded to two significant digits or the hundredth position.

Table 4.3 presents scan MDAs for a surveyor velocity of 1.0 m/s. Scan MDAs for the various radionuclides and field conditions follow the same trend as the values under the slower surveyor velocity. Unsurprisingly, the higher surveyor velocity yields a higher scan MDA relative to a surveyor velocity of 0.5 m/s—by a factor of approximately 1.4.

Table 4.3. DRP scan MDA for various scan conditions and a surveyor velocity of 1.0 m/s (µCi)

Particle Depth in Soil	Radionuclide and Ground-to-Detector Distance							
	Co-60		Cs-137		Th-232		Am-241	
	7.5 cm	10 cm	7.5 cm	10 cm	7.5 cm	10 cm	7.5 cm	10 cm
Optimistic Scenario (Figure 2.1a)								
Surface	0.17	0.21	0.33	0.41	0.08	0.11	0.70	0.90
7.5 cm	0.31	0.35	0.67	0.76	0.23	0.26	–	–
15 cm	0.61	0.68	1.6	1.7	0.59	0.65	–	–
30 cm	2.4	-	8.3	-	-	-	-	-
Pessimistic Scenario (Figure 2.1b)								
Surface	0.74	0.75	1.5	1.5	0.39	0.39	3.4	3.5
7.5 cm	1.4	1.3	3.5	3.3	1.3	1.2	-	-
15 cm	2.3	2.3	6.9	6.5	2.7	2.5	-	-
30 cm	6.9	-	28.2	-	-	-	-	-

"–" indicates the calculation shows the DRP cannot be identified during scans.
All values rounded to two significant digits or the hundredth position.

Tables 4.1 to 4.3 show that a ground-to-detector distance of 10 cm yields a slightly lower scan MDA than the 7.5 cm height, for the pessimistic scenario when the DRP is present at depth. A couple factors may explain this phenomenon. One, is that under the pessimistic scenario, the detector response is calculated based on the tail of the efficiency curve, where the fit of the log-logistic curve is not as robust as it is for smaller offset values. The other likely cause is that a DRP at depth must travel through a greater distance of soil to reach the detector volume when the ground-to-detector distance is lower. That is, there is more soil attenuation under when the detector is positioned at a height of 7.5 cm than 10 cm. The magnitude of this distance depends on the detector offset from the DRP—a higher offset yields more attenuation. Further review of the raw efficiency data indicate that the latter factor is the more likely cause. Efficiency data for particles at depth is higher for the 10 cm than for the 7.5 cm ground-to-detector distance, with the magnitude of the difference proportional to the detector offset.

4.2 RESPONSE COMPARISON FOR MICROSHIELD ANALYSIS

Scan MDAs calculated using the MicroShield method are presented in Table 4.4 for a ground-to-detector distance of 7.5 cm. The corresponding MCNP-calculated scan MDA is also presented in Table 4.4. In general, the MicroShield-calculated values are larger than the MCNP-calculated value, except for the pessimistic scenario where the DRP is located on the surface. MicroShield derived efficiency curves yield a higher scan MDA than the MCNP counterpart for all scenarios except for the pessimistic scenario with the particle located on the soil surface. This difference is expected because MCNP accounts for low-energy photons from scattering, which are more efficiently detected by the NaI detector. Whereas MicroShield only considers primary photons when estimating buildup (Ablequist 2014).

Table 4.4. Scan MDA Calculations using MicroShield; Ground-to-Detector Distance of 7.5 cm (µCi)

Particle Depth in Soil	Co-60			Cs-137		
	MicroShield	MCNP	Ratio[a]	MicroShield	MCNP	Ratio[a]
Optimistic Scenario (Figure 2.1a)						
Surface	0.15	0.12	1.2	0.27	0.23	1.1
7.5	0.40	0.22	1.8	0.76	0.47	1.6
15	0.91	0.43	2.1	1.8	1.1	1.7
30	3.9	1.7	2.3	10	5.9	1.7
Pessimistic Scenario (Figure 2.1b)						
Surface	0.44	0.52	0.8	0.82	1.0	0.8
7.5	1.1	0.99	1.1	2.2	2.5	0.9
15	2.0	1.7	1.2	4.9	4.9	1.0
30	6.6	4.9	1.4	21	20	1.0

[a] Ratio is the MicroShield value to MCNP value, i.e. (MicroShield/MCNP)

Table 4.5 presents MicroShield-calculated scan MDAs for a ground-to-detector distance of 10 cm; as with the previous table, the corresponding MCNP-calculated values are presented as well. The relationship between the two sets of values are similar to those of the 7.5 cm ground-to-detector distance.

Table 4.5. Scan MDA Calculations using MicroShield; Ground-to-Detector Distance of 10 cm (µCi)

Particle Depth in Soil	Co-60			Cs-137		
	MicroShield	MCNP	Ratio[a]	MicroShield	MCNP	Ratio[a]
Optimistic Scenario (Figure 2.1a)						
Surface	0.19	0.15	1.3	0.35	0.29	1.2
7.5	0.47	0.25	1.9	0.88	0.54	1.6
15	1.01	0.48	2.1	2.0	1.21	1.7
30	4.2	-	-	11	-	-
Pessimistic Scenario (Figure 2.1b)						
Surface	0.46	0.53	0.9	0.84	1.05	0.8
7.5	1.0	0.94	1.1	2.0	2.31	0.9
15	1.9	1.60	1.2	4.5	4.59	1.0
30	6.5	-	-	20	-	-

[a] Ratio is the MicroShield value to MCNP value, i.e. (MicroShield/MCNP)

As shown in the previous section, MicroShield derived scan MDAs for a ground-to-detector distance of 10 cm are slightly higher than those for the 7.5 cm detector height. This provides further evidence that the difference is due to differing levels of soil attenuation between the two detector heights.

4.3 MCNP QC Results

Figure 4.1 plots measured responses and MCNP-modeled results for the Co-60 offset experiment. Each line corresponds detector efficiency—in units of counts/decay—as a function offset distance (δ). Results show good agreement in the shape of the curves, suggesting the MCNP model effectively mimics real-world conditions. Results also show that the MCNP model slightly over-estimates detector response relative to the measured values, suggesting some error in one or both methods. Identifying modeled errors is difficult; however, sources of error include the fact that the Co-60 is not a point source and the surface is a countertop (some backscatter?), not soil. It would be preferrable that the modeled values over predict efficiency as this would yield more conservative [higher] scan MDAs. Furthermore, the test source was not NIST-Traceable, therefore there is

additional uncertainty within efficiency calculations for the real-world detector. Another factor influencing this comparison is that the modeled detector is an "ideal" NaI detector. Varying factors—including detector age and instrument settings—can influence the response of the real-world NaI detector (NRC 2020). The difference discussed herein may be addressed by measuring a small sample of NaI detectors and developing a factor to correct the MCNP model. The MARSSIM practitioner will need to assess project data quality objectives before implementing a specific scan MDA calculation paradigm for DRPs.

There are several known factors that contribute error to the scan MDA calculations. Sources of error include, but are not limited to, the following:

- Selected values of *d'* and *p* in *MDCt* calculations—a project is encouraged to select inputs that are consistent with project-specific data quality objectives,
- A non-point source used in the Co-60 offset experiment, noting that DRPs are modeled as point sources,
- A wooden table used in the Co-60 offset experiment, noting that DRPs are modeled to be on or under layers of soil, not wood, and
- Surveyors are unlikely to pass the detector directly over the DRP, so selecting values between "optimistic" and pessimistic scan MDAs may be prudent.

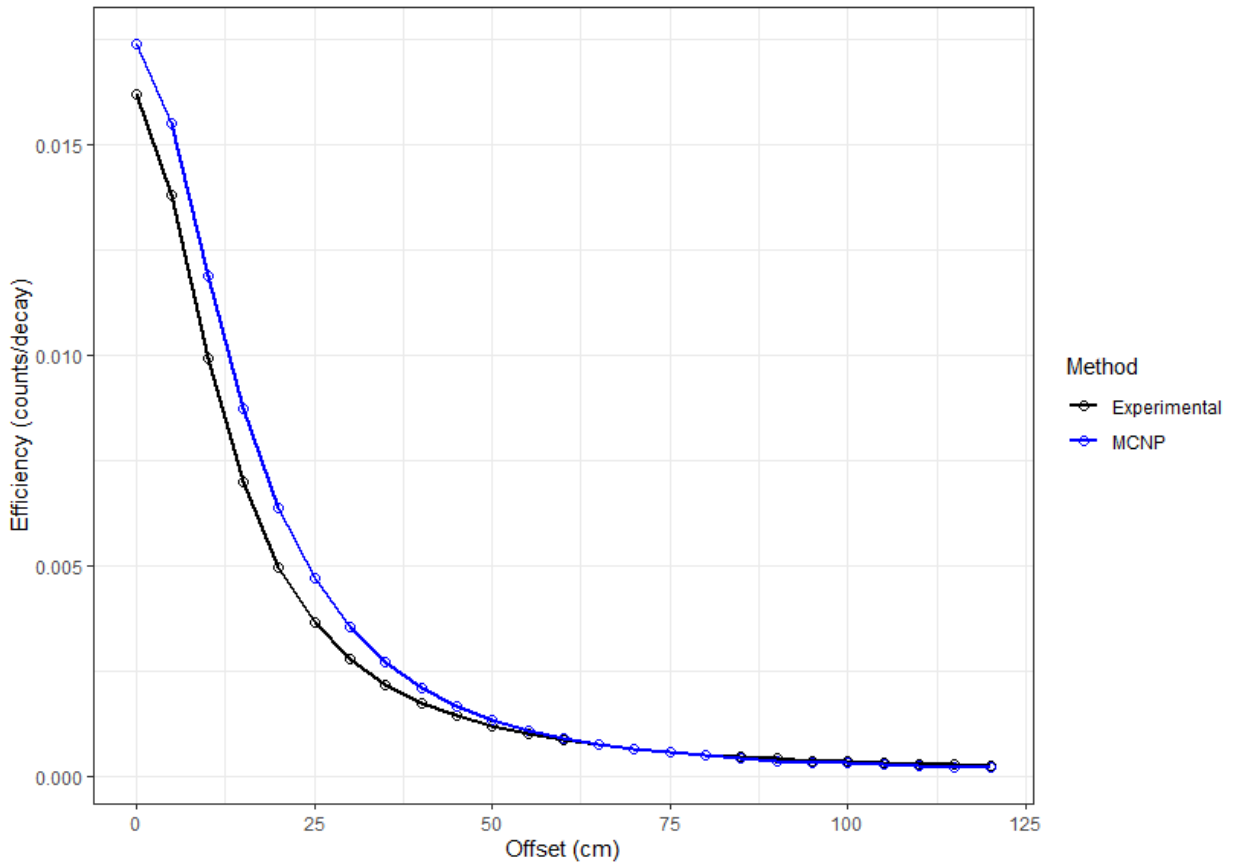

Figure 4.1. Experimental and modeled relative responses for a Co-60 source with increasing offsets

5. CONCLUSIONS

MCNP was used to estimate the scan MDA for a series of radionuclides (Co-60, Cs-137, Th-232, and Am-241), detector heights (7.5 cm and 10 cm), and soil depths (0 cm, 7.5 cm, and 15 cm). A series of offsets was also considered to evaluate the scenarios where the detector either passes over the source (the optimistic scenario) or passes near, but not over, the source (pessimistic scenario). An experiment was also conducted with a small Co-60 source to compare the validity of the model by comparing empirical and hypothetical detector responses.

Results for the surveyor paradigm show that more activity is required when gamma radiation energy and intensity is low—this is expected. Specifically, the Am-241 DRP will not be detectable, according to the model, if covered in 7.5 cm (~3 inches) of soil and Th-232-series gammas are shielded more effectively than high-energy, high-yield gammas from, for example, Co-60—again this is expected. These expected results demonstrate that the model performs in a manner consistent with expected real-world conditions. It is also observed that the pessimistic MDA values are

approximately two times the optimistic MDA values. Given it is unlikely that a surveyor will pass the detector directly over the DRP, it may be prudent for planners to select scan MDA values between optimistic and pessimistic values.

In general, the scan MDA calculation shows that the lowest scan MDAs occur when the detector is positioned closest to the ground, the surveyor walks as slow as possible, the DRP is positioned on the surface, and the detector passes directly above the DRP. Survey designers should consider surveyor velocity, ground-to-detector distance, and potential soil-cover depth when planning a final status survey. A surveyor velocity of 0.25 m/s may be unreasonable in real-world applications, i.e. surface terrain prevents the surveyor from traversing this slowly. However, optimization of the survey design may include a scan MDA based on a surveyor velocity of 0.25 m/s for small areas receiving follow-up investigations. Similarly, a reasonable ground-to-detector distance may be established for routine scanning that enables the surveyor to avoid hitting the detector on debris. This source-to-detector distance may be reduced in areas requiring a higher level of scrutiny. Because the thickness of soil cover greatly influences the scan MDA, DRP investigation surveys should occur prior to any site actions that have the potential to re-distribute DRPs into deeper soil strata.

Finally, modeled NaI detector efficiency results are similar to, though slightly greater than, experimental results when considering detector responses from a Co-60 source. The fact that modeled results generally mimic experimental results gives validity to the overall method.

6. REFERENCES

Ablequist 2014. *Decommissioning Health Physics a Handbook for MARSSIM Users, Second Edition.* Taylor & Francis Group. Boca Raton, Florida.

NRC 2020. *Minimum Detectable Concentrations with Typical Radiation Survey for Instruments for Various Contaminants and Field Conditions.* NUREG-1507 Revision 1. U.S. Nuclear Regulatory Commission. Washington, D.C. August.